

Effects of wide-base tires on low-volume pavement structures



Jérôme Fachon
Guy Doré
Damien Grellet
Romain Marcel

Groupe de recherche en ingénierie des chaussées

www.gci.ulaval.ca

July 2008





Contents

INTRODUCTION 4

1. PROJECT PRESENTATION 4

 1.1 EXPERIMENTAL SITE 4

 1.2 EXPERIMENTAL PROGRAM..... 4

 1.2.1 *Horizontal strain sensors* 6

 1.2.2 *Vertical strain sensors*..... 9

 1.2.3 *Moisture and temperature sensors* 10

 1.3 ADDITIONAL EQUIPMENT 10

 1.4 THE TRUCK..... 12

2. TESTING PROCEDURE 13

3. DATA ANALYSIS..... 14

 3.1 RELIABILITY OF THE TEST RESULTS 16

 3.1.1 *Comparison between valid pass signals* 16

 3.1.2 *Transverse sensors characteristics*..... 17

4. DATA ANALYSIS..... 18

 4.1 EFFECT OF PRESSURE VARIATION 18

 4.2 DIFFERENCES BETWEEN TWIN TIRES AND WIDE-BASE TIRES 20

5. SUMMER TESTING PROGRAM 21

6. CONCLUSION 21

 ANNEX 1. TRUCK CHARACTERISTICS 23

 ANNEX 2. TRIALS MATRIX 26

 ANNEX 3. TEST RESULTS 27

Figures caption

Figure 1: Sensors ready for installation in the pavement..... 5

Figure 2: instrumentation 6

Figure 3 : Installation of a sensing element at the base of an asphalt core..... 7

Figure 4: Calibration bench for AC instrumented cores 7

Figure 5: calibration coefficient obtained from sensor calibration..... 8

Figure 6: sample fixed in the pavement 8

Figure 7: Schematic illustration of the 100mm instrumentation core in operating conditions.9

Figure 8: installation of the vertical strain sensors.9

Figure 9: Moisture and temperature sensors10

Figure 10: Temperature control blanket.....11

Figure 11: the steering guide.....11

Figure 12: Tire position on the gauges as recorded by the video camera.12

Figure 13: Test vehicle.....12

Figure 14: example of an original graph14

Figure 15: signal obtained after data processing for one sensor.....15

Figure 16: Sensors numbered15

Figure 17: Valid measures with wide tires and pressure 100/100/120Psi on the 100mm section16

Figure 18: Valid measures with wide tires and pressure 100/100/120Psi on 100mm section17

Figure 19: example of three valid transverse strain measurements.....17

Figure 21: Pressure effect for wide tires (over-inflated/normally-inflated).....19

Figure 22: Pressure effect for wide tires (normally-inflated/under-inflated)20

Figure 23: Comparison between twin and wide-base tires.....21

Introduction

The goal of the study presented in this report is to assess the effect of wide-base tires on low-volume pavement structures. The first series of tests took place during spring, at the Laval University Road Experimental Site (SERUL) in “Forest-Montmorency”, 75 km north of Quebec City.

The study involves the comparison of the effect of regular twin tires and wide-base tires based on strains measurements under a moving wood-harvesting truck.

1. Project presentation

1.1 Experimental site

The spring tests were conducted at the SERUL, a test road specially designed to test the effects of heavy vehicles on pavement structures. The site is located 75 km north of Quebec City.

This site was constructed to study:

- The behavior of pavement structures and materials subjected to loading in severe climatic conditions.
- The effect of heavy vehicles on pavement structures.

The test section dedicated to studies on the effects of heavy loads (AVL section) is divided in four sub-sections with varying thicknesses of the surfacing layer. Three sections have asphalt concrete surfaces with thicknesses of: 100 mm, 200 mm, and 50 mm. The fourth section has been surfaced using a surface treatment and an ultrathin slurry coating having a total thickness of 25 mm. Since the focus of the study is on low-volume pavement structures, the tests were conducted on the 100mm, the 50mm and surface treated sections.

1.2 Experimental program

The sections are instrumented to measure horizontal strains in the asphalt concrete and vertical strains in the granular base layer. These mechanical responses are considered to be relevant for the assessment of tire type effects on pavements. Fiber optic sensors

were used for strain measurements. In addition, moisture sensors were installed in the granular base layer of all sections and temperature sensors were installed in the asphalt concrete layer of the three relevant sections.

Figure 1 illustrates the sensors used in each section and the installation layout. The horizontal strain sensors were installed in 50 mm core holes while the vertical strain sensors, the moisture sensors and the temperature sensors were installed through 150 mm core holes.

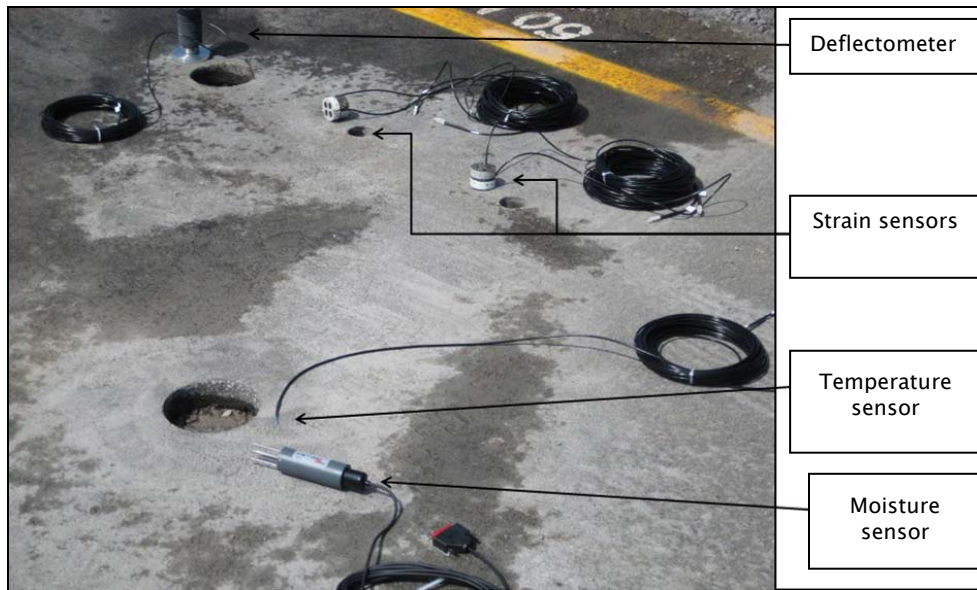


Figure 1: Sensors ready for installation in the pavement

The surface treated pavement section was instrumented using a vertical strain sensor only. In each other section (100mm and 50mm), two 50 mm holes cored 500 mm apart were used to install two instrumented cores, each one including two perpendicular strain sensors. Figure 2 illustrates the instrumentation layout in each AC section.

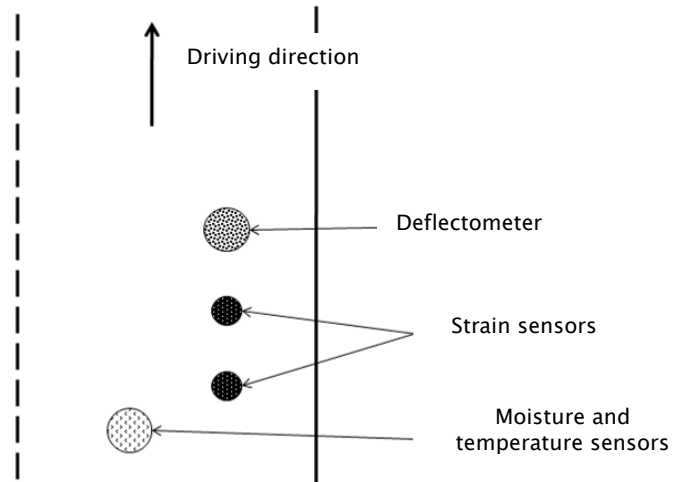


Figure 2: instrumentation

1.2.1 Horizontal strain sensors

Strain sensors are used to measure horizontal strains at the bottom and at shallow depth (25 mm) in the asphalt bound layer. The sensors were assembled at Laval University. Each sensing element, including two perpendicular optic fiber strain gauges, is assembled using epoxy glue at the base of a machine-carved AC core. The diameter of the instrumented cores is minimal, reducing the risk of perturbations in asphalt mechanical behavior. Figure 3 illustrates the cores and the sensing element installed at the bottom of a core.

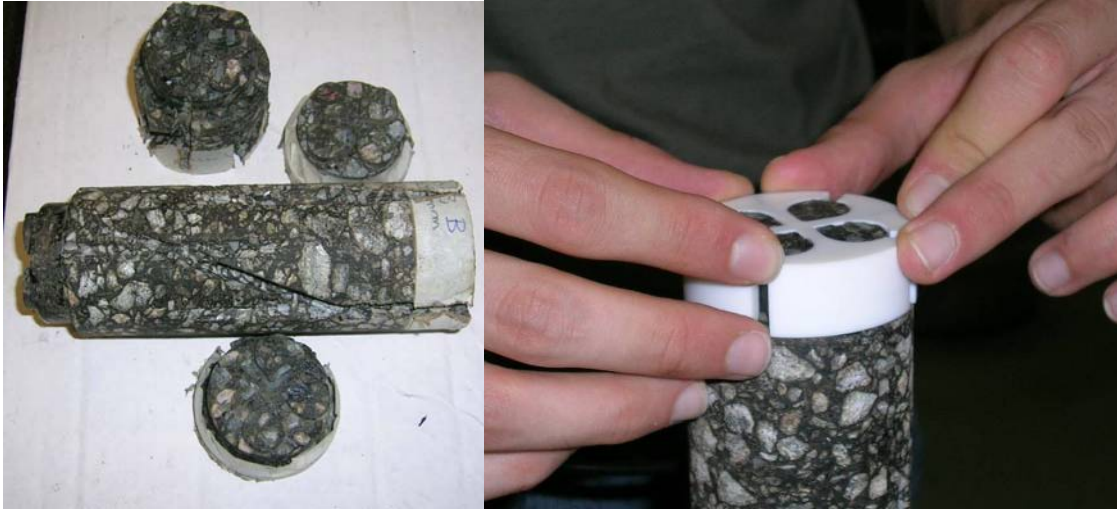


Figure 3 : Installation of a sensing element at the base of an asphalt core

The instrumented cores for the 100mm AC section include two sensing elements in order to allow for the measurement of horizontal strains at the bottom and at shallow depth in the layer. The 50mm AC section has a sensing element at the bottom of the layer only due to the insufficient thickness of the layer.

Once assembled, sensors are calibrated as illustrated in figure 4.

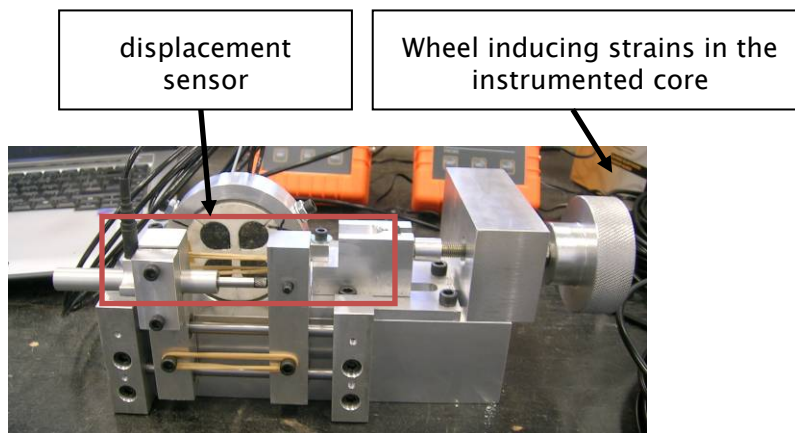


Figure 4: Calibration bench for AC instrumented cores

Samples are placed in a calibration bench. They are on a steel ring used to induce horizontal strains in the sensors. Strains measured by the sensor are compared to strains inferred from diameter variations measured using a high precision displacement transducer. A calibration coefficient can be obtained from the correlation curve as indicated in figure 5.

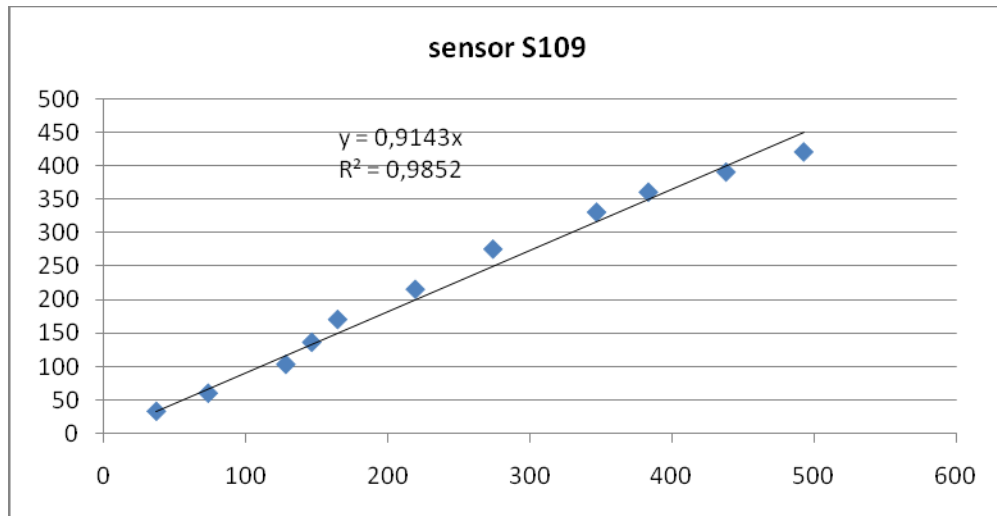


Figure 5: calibration coefficient obtained from sensor calibration

The example shown in figure 5 indicates a calibration coefficient 0.9143 for sensor S-109.

As illustrated in figure 6, instrumented cores are then placed in the core hole and fixed using epoxy glue.



Figure 6: sample fixed in the pavement

Figure 7 shows a schematic representation of the instrumentation core to better illustrate the position of the sensors in the asphalt bound layer.

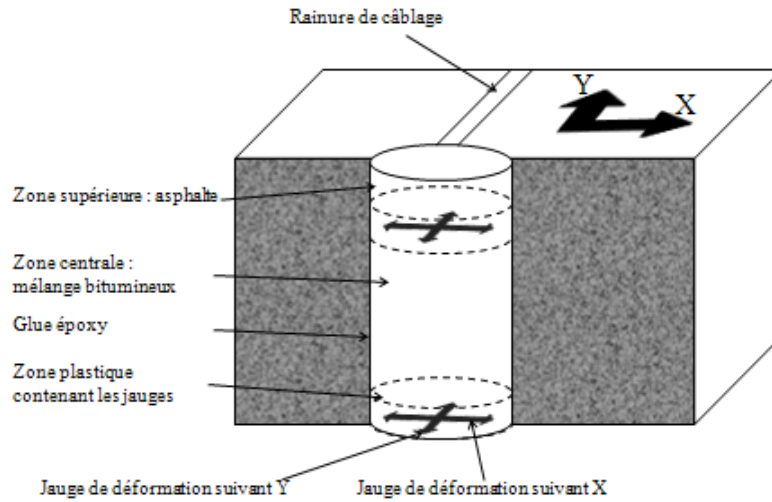


Figure 7: Schematic illustration of the 100mm instrumentation core in operating conditions.

Sensors along the X axis measure longitudinal strains while those along the Y axis measure transverse strains. In this case, the strains are measured at two different levels (at shallow depth and at the bottom of the bound layer).

1.2.2 Vertical strain sensors

The vertical strain sensors are designed to measure strains in the unbound granular bases. It is positioned such as the top of the sensor is just below the bottom of the asphalt bound layer.



Figure 8: installation of the vertical strain sensors.

1.2.3 Moisture and temperature sensors

These components were added to the study to improve our ability to analyze the data by measuring moisture content in the base layer and temperature in the asphalt concrete layer. As illustrated in figures 1 and 2, these sensors were located slightly outside the wheel path. Moisture is measured using DeltaT ML2X probes (figure 9) which measure volumetric water content using TDR technology. Temperature in the AC layer is measured using fiber optic temperature sensors.

The information given by these sensors can help refine theoretical modeling of the pavement system to improve data analysis.



Figure 9: Moisture and temperature sensors

1.3 Additional equipment

- Thermal control blanket: An insulated blanket has been designed to help controlling the surface temperature at a constant level during a series of tests. The thermal blanket is a 2,5 m X 2,5 m insulated blanket covering 2 circuits of flexible pipes in which a refrigerated (heated) fluid is circulated. Each circuit is linked to a cooling (heating) unit each one having a 1000 W cooling (heating) capacity. The blanket is placed in the instrumented portion of the pavement every morning before the beginning of the tests and is removed only for the duration of a truck pass (approximately 15 s). The surface temperature was set to be at $10^{\circ}\text{C} \pm 2^{\circ}\text{C}$ for spring tests. Temperature is controlled using the thermal sensor in each section.



Figure 10: Temperature control blanket

- Steering guide: In order to guide the truck on the sensor with a reasonable accuracy, a guiding system has been developed and is installed on the truck to provide a reference for the driver. The steering guide is composed of 2 articulated aluminum rods adjusted so that the guiding reference is just above the lane separation line.



Figure 11: the steering guide

Position marker and camera: To accurately record the position of the tire relative to the sensors during the course of a test, a position marking plate is placed just before the sensors. The position of the tire on the marker is recorded using a digital video camera. It is thus easy to measure the exact position of the tire on the gauges for each truck pass. Figure 12 shows the position of the tire on the

marker for two truck passes. The three orange lines on the marker represent the tolerance zone. The left picture shows a valid pass as the tire edge is on the center orange line, while the picture on the right shows an invalid pass as the tire edge is beyond the orange tolerance line.



Figure 12: Tire position on the gauges as recorded by the video camera.

1.4 The truck

A Kenworth/trailex wood harvesting truck has been used for the tests. It has been loaded with logs to reproduce real conditions. Detailed information on wheel loads are given in annex 1.



Figure 13: Test vehicle

2. Testing procedure

For each test condition, three valid truck passes were required. A truck pass was considered valid when the tire was within 50 mm of the target. The data set corresponding to the tire position which was the closest to the target was used for the analysis. As specified in the terms of reference of the project, the tests were conducted for three AC thicknesses (100mm, 50mm and surface treatment) and three tire pressures (840, 700 and 560 kPa). Considering the truck characteristics and the short time frame for spring testing, it has not been impossible to test at different load levels. After the full sequence of test with the dual tires, the wide-base tires have been installed on the truck for an additional sequence of tests. Analysis will focus on the tire effect for equal pressure on each test section.

For each test, the truck speed was maintained at 30 km/h. Temperature and moisture were frequently measured and the thermal control system was adjusted when required.

Gauges readings were done using an 8-channel "Prosens" fiber optic signal conditioner. Measurements were made with an acquisition frequency of 500 Hz (a 3 seconds test = 1500 data points per sensor).

3. Data analysis

The graphics presented generally include several signals for comparison purposes. Each signal represents the reading of a sensor during a truck pass. Readings are reported in μ strains as a function of time (s).

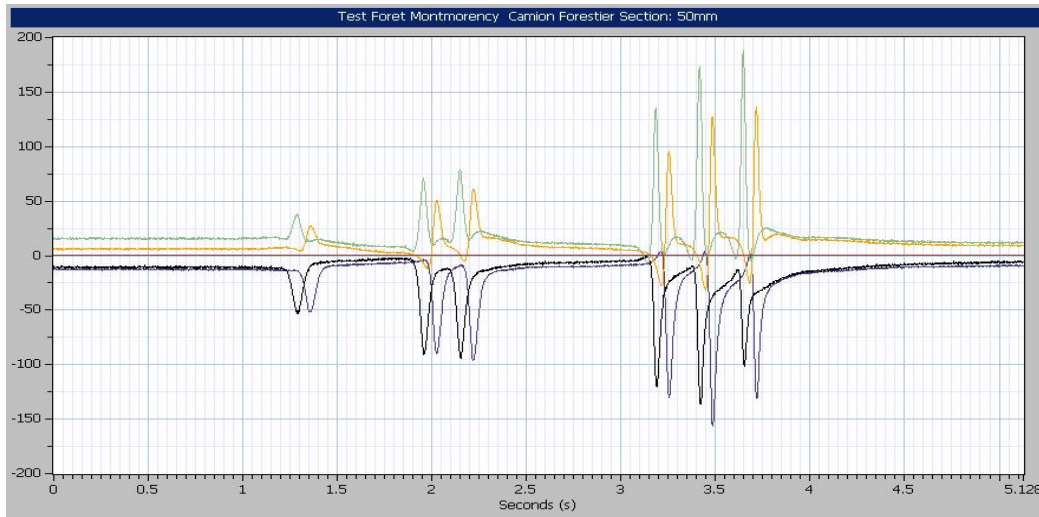


Figure 14: example of an original graph

Each data point is recorded in a file allowing for data cleansing prior to analysis. A computer program has been developed by our research group to facilitate this operation. The following treatment is done of the raw data set:

- The signal is adjusted to set the initial strain reading at 0, right before the test axle group (the trailer tridem axle group in this study). This operation allows removing any residual strains caused by the steering and driving axle groups.
- The signal is also corrected in order to superpose the first peak if the test axle group in order to facilitate signal comparison.

Figure 15 shows a processed signal.

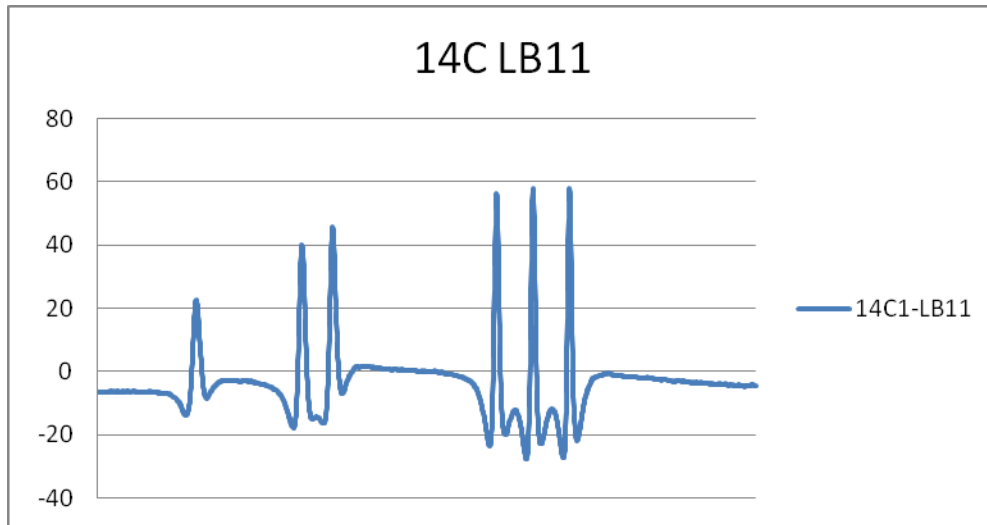


Figure 15: signal obtained after data processing for one sensor

The computer program also separates signals recorded by each individual sensor making it easier to select the signals to be compared.

Sensors have been numbered from 1 to 12 as shown in Figure 16: Sensors numbered. Sensors labeled “D” are vertical strain sensors while others are horizontal strain sensors.

⊗ ⊗ ⊗ ⊗ D12 11 10 9 Section 100 mm	⊗ ⊗ ⊗ ⊗ D8 7 6 5 Section 200 mm	⊗ ⊗ ⊗ D4 3 2 Section 50 mm	⊗ D1 Enduit
--	---	--	-----------------------

Figure 16: Sensors numbered

Note that the 200mm section is not used in this study.

Table 1 summarizes the labeling convention used to distinguish the various types of sensor used in one instrumented core.

Table 1: sensor labeling convention

Letter	definition
L	Longitudinal (driving direction)
T	Transverse (perpendicular)
H	Top of the pavement
B	Bottom of the pavement
D	Deflectometer (vertical strain sensors)
1 à 12	Hole number

For example, sensor LB11 measures longitudinal strains at the bottom of the bound layer, in hole number 11 (i.e. on the 100mm section).

Each test has a specific test number. The number is structure as follows: Number–letter–number (e.g. 27C1). The first number is the series number (one for each test condition), the letter C designates the test vehicle (“Camion”). The last number corresponds to the pass number for a specific test condition.

3.1 Reliability of the test results

3.1.1 Comparison between valid pass signals

Figures 17 and 18 show a comparison between the three signals obtained for the valid passes in one test series for two different sensors.

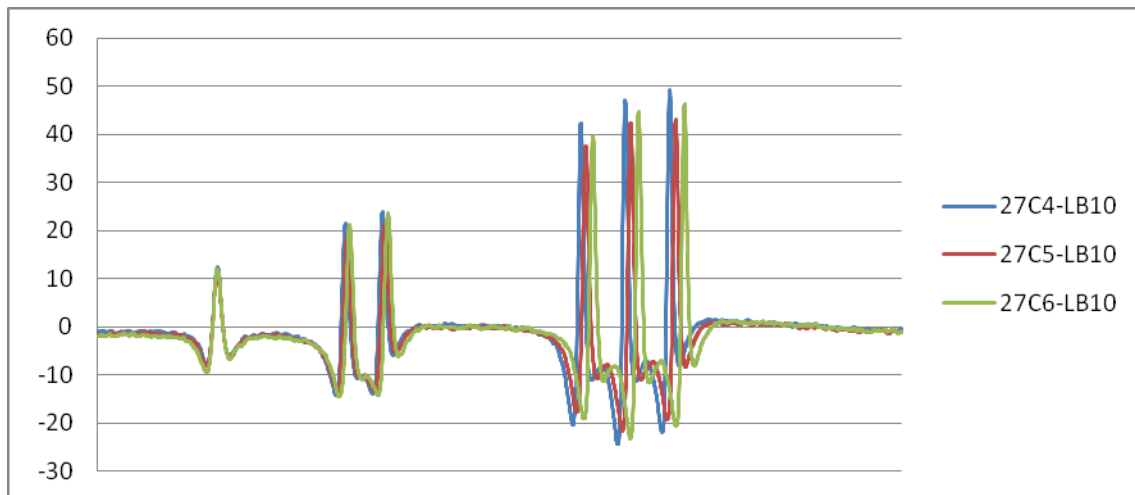


Figure 17: Valid measures with wide tires and pressure 100/100/120Psi on the 100mm section

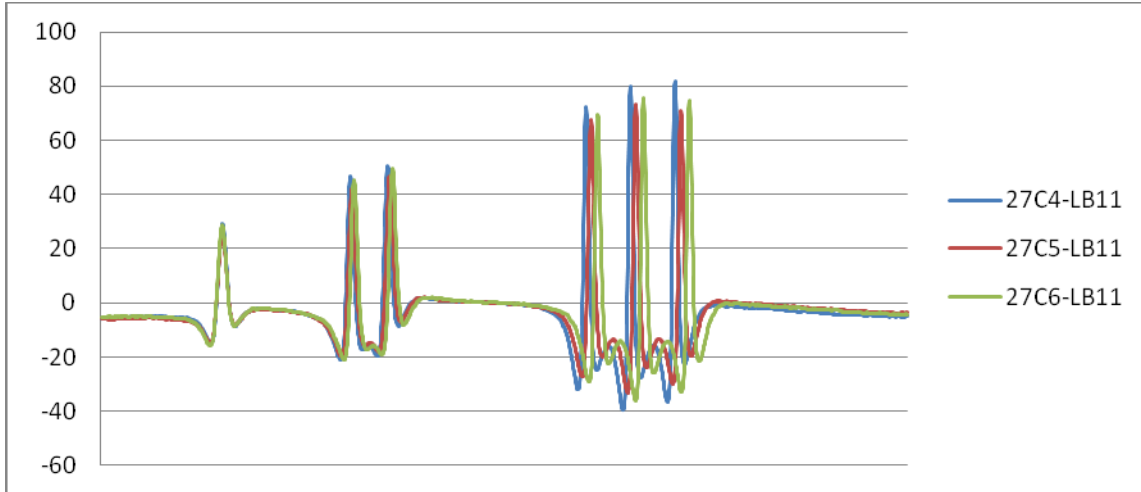


Figure 18: Valid measures with wide tires and pressure 100/100/120Psi on 100mm section

It can be concluded from these figures that there is no significant difference between strain readings for a given sensor if the tire is within the 50 mm offset tolerance. It can be seen however that measured strain can differ between sensors. The difference is likely to be corrected by the application of the calibration factor to the strain reading (calibration factors are applied to peak height and not to the signal).

3.1.2 Transverse sensors characteristics.

As illustrated in figure 19, transverse strain sensors are more sensitive to offset within the tolerance zone.

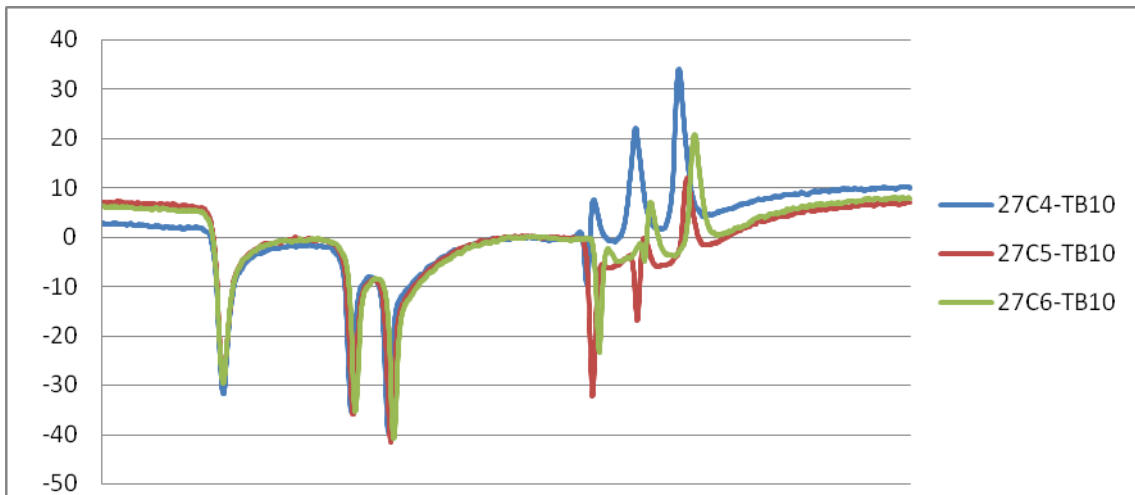


Figure 19: example of three valid transverse strain measurements

Table two provides the offset for each-one of the passes illustrated in figure 19.

Table 2 : Offset for the three axles for the valid passes of series 27

Serie	Tridem offset		
	wheel 1	wheel 2	wheel 3
27C4	0	10	50
27C5	-10	10	40
27C6	-20	10	40

It is clear from the comparison that all three tests were conducted with the truck passing on the gauges with a slight angle. The pass where the position of the axles is the closest from the target correspond to the highest transverse tensile (negative values) strains measured during that series. The transverse strains will thus be used to help selecting the best truck pass for data analysis.

This approach had been applied for every test series. The signals listed in table 3 were used for the preliminary analysis described in section 4 of this report in this report.

Table 3 : Synthesis of the selected trials

Forest truck	14C6	15C2	16C14	17C3	18C4
	19C10	20C4	21C2	22C4	24C4
	25C5	26C6	27C5	28C6	29C2

4. Data analysis

Due to the variability of many experimental factors, changes in pavement response associated with a change in an experimental variable are variable as well. In order to represent this variability in the experimental relationship, the preliminary results of this study are presented in terms of variation distribution. Effect of tire pressure is presented in figure 21 and 22. For the purpose of this preliminary report, the effect of pressure is assessed by comparing all passes at the reference pressure (100 psi or 700 kPa in this study). Results are represented in terms of frequency occurrence of a given relative difference magnitude. For example, in figure 21, it can be seen that in three tests, the 120 psi inflation caused 20% more strain than the test with similar condition with the 100 psi tire inflation. In two other cases, the strains were 10% less.

4.1 Effect of pressure variation

The effect of tire pressure has thus been assessed by comparing the peak strains measured under the last axle of the tridem for all tests done with the wide-base tires. Figure 21 shows the comparison between the tests conducted at 120 psi and tests conducted in similar conditions with tires at 100 psi. Negative values mean that tires with 120 inflation pressure are inducing more strains than the tires with a 100 psi inflation pressure.

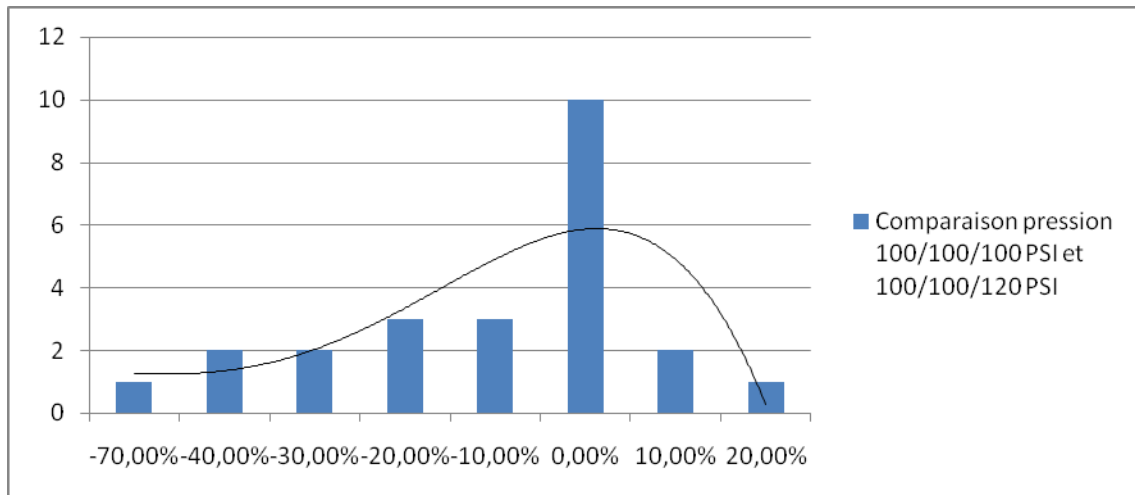


Figure 20: Pressure effect for wide tires (over-inflated/normally-inflated)

It can be observed on figure 21 that even if more tests have shown more damage with tire inflation of 120 psi, there is no significant difference between the 120 psi and the 100 psi inflation pressure. It should be noted however that this statement is not supported by a detailed statistical analysis at this point. The comparison between the 100 psi and the 80 psi however show a clear difference between two inflation pressures. Figure 22 shows that tires with 80 psi inflation pressure tend to cause between 10 and 20% less strains than the 100 psi inflation pressures.

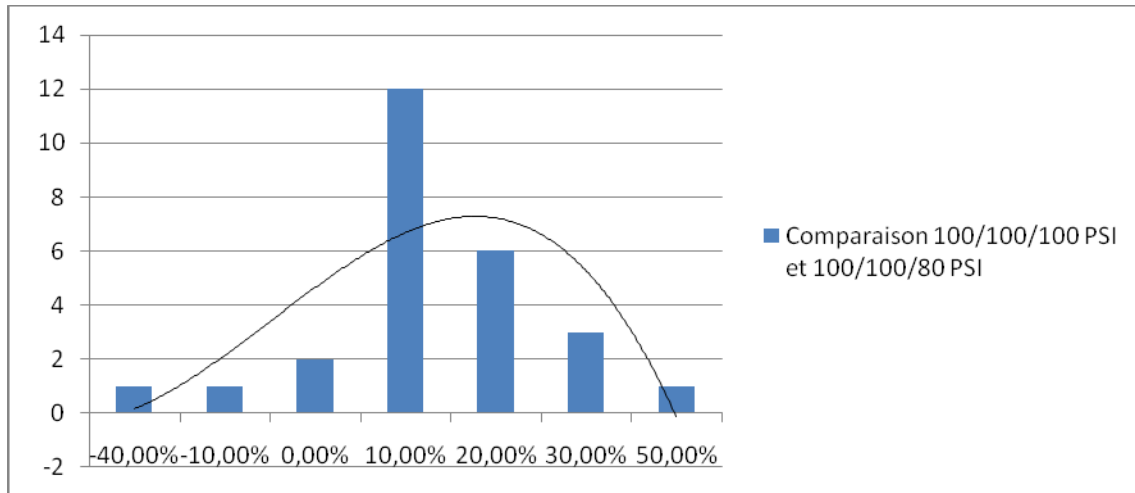


Figure 21: Pressure effect for wide tires (normally-inflated/under-inflated)

The following table summarizes the results of the analysis of tire pressure effects.

Tableau 1: Differences in strains associated with the pressure variation

Inflation layout	Effects on deformations
Twin tires 100/55	20%
Wide tires 100/120	0%
Wide tires 100/80	15%

4.2 Differences between twin tires and wide-base tires

In this section, strains caused by twin tires are compared with those caused by wide-base tires. In the following analysis, The 100 psi pressure is used for the comparison.

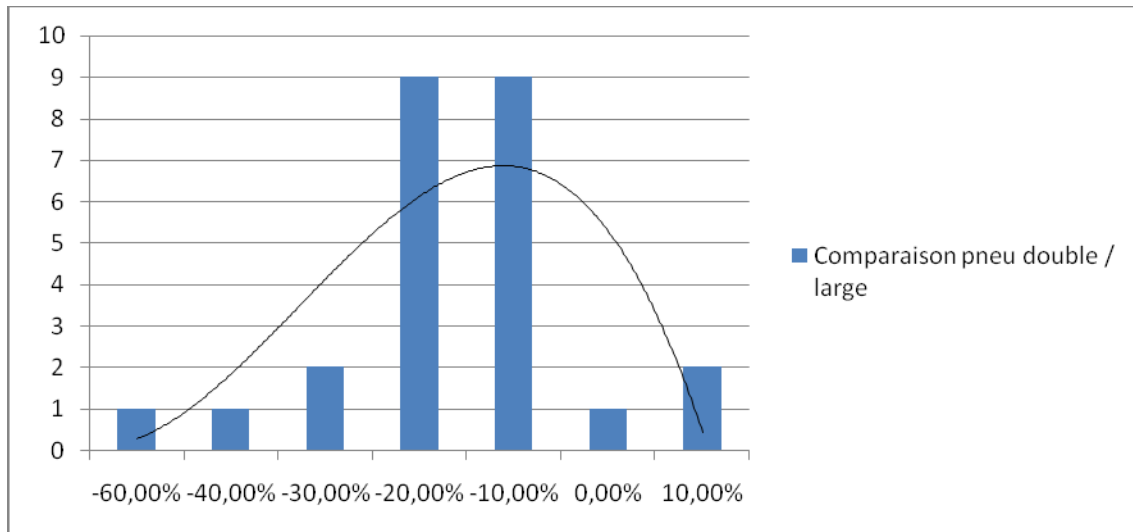


Figure 22: Comparison between twin and wide-base tires

The preliminary analysis of the relative effect of wide-base tire shows a significant difference between the two types of tires. Based on all horizontal strains measured at the base of the test sections, the wide-base tire appear to cause between 10 and 20% more strains that the dual tires with equivalent loading conditions.

5. Summer testing program

The summer test program will be conducted according to the terms of reference. In additions to the spring test conditions, the summer program will include the effect of different load levels. As part of summer testing, tire print measurements and moisture measurements in all pavement layers will also be conducted.

6. Conclusion

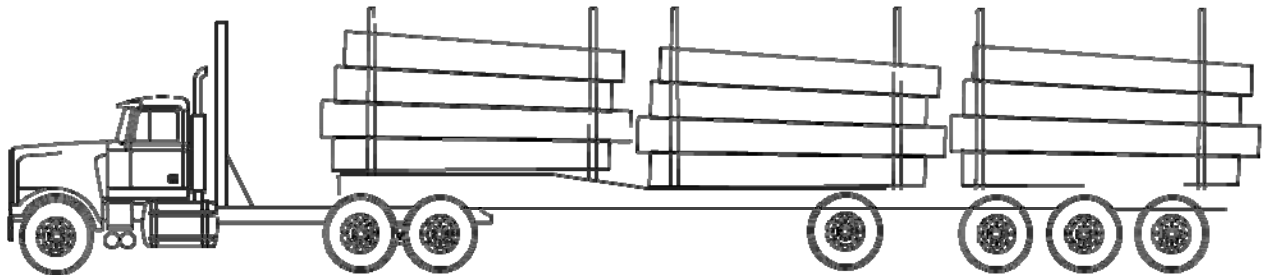
In general, the spring testing program has been successful. Most of the conditions specified in the terms of reference have been tested. For logistic reasons, it has not been possible to test with variable load conditions and because of unusual climatic conditions, tests have been conducted with a greater thaw depth than expected. The fall testing program has allowed adjusting the testing protocol and all changes made greatly improved the quality of the experimental program.

Based on a summary analysis of the spring test results, it appear that wide-base tire induce more strains at the bottom of the asphalt pavements than dual tires. Induced strains are reduced when wide-base tires are inflated at pressures lower than 100 psi.

ANNEX 1. *Truck characteristics*

Forest truck characteristics

Truck	
Owner	Daniel Tardif
Make	Kenworth
Model	T800
Color	Orange
Trailer	
Make	Trailex



Load by wheel shaft group Date : 6 may 2008 (14h00)		
Simple wheel shaft	Double wheel shaft	Triple wheel shaft
5 460 kg	17 900 kg (axial load= 8 950 kg)	25 650 kg (axial load = 8 550 kg)

Load by wheel shaft Date : 7 may 2008		
	Driver side	Passenger side
double wheel shaft #1 (tires 3-6)	4.55 t	4.61 t
double wheel shaft #2 (tires 7-10)	4.35 t	4.45 t
Triple wheel shaft #1 (tires 19-22)	4.21 t	4.6 t
Triple wheel shaft #2 (pneus 23-26)	3.95t	4.55 t
Triple wheel shaft #3 (tires 27-30)	4.0 t	4.45 t

Spécifications pour bandes de roulement: X One[®] XDA-HT™ Plus

Dimension	Gamme de charge	Numéro de catalogue	Profondeur de bande de roulement (32e)	Vitesse maximale (mi/h)	Rayon sous charge		Diamètre hors tout		Largeur hors tout		Jantes approuvées	Entraxe min. entre jumelés		Tours/mille	Charge maximale (pneus simples)				Charge maximale (pneus jumelés)			
					po	mm	po	mm	po	mm		po	mm		lb	psi	kg	kPa	lb	psi	kg	kPa
445/50R22.5	L	38873	28	75	18.7	475	40.5	1028	17.1	435	14.00			514	10200	120	4625	830				
455/55R22.5	L	31697	28	0	19.6	498	42.5	1078	17.6	448	14.00			490	11000	120	5000	830				

Specifications for Tread Design: XZY[®] 3

Size	Load Range	Catalog Number	Tread Depth 32nds	Max Speed mph	Loaded Radius		Overall Diameter		Overall Width		Approved Rims	Min. Dual Spacing		Revs per Mile	Max. Tire Load Single				Max. Tire Load Dual			
					in.	mm.	in.	mm.	in.	mm.		in.	m		lbs.	psi	kg.	kPa	lbs.	psi	kg.	kPa
11R22.5	G	84455	24	65	19.6	498	41.8	1061	11.3	288	8.25, 7.50	12.5	318	496	6175	105	2800	720	5840	105	2650	720
11R22.5	H	80927	24	65	19.6	498	41.8	1061	11.3	288	8.25, 7.50	12.5	318	496	6610	120	3000	830	6005	120	2725	830
12R22.5	H	47947	24	65	20.1	509	42.9	1089	11.4	290	8.25, 9.00	13.2	335	483	7390	120	3350	830	6780	120	3075	830
315/80R22.5	L	40200	23	65	19.8	502	42.9	1088	12.5	318	9.00, 8.25	13.8	351	486	9090	130	4125	900	8270	130	3750	900
11R24.5	G	47945	24	65	20.5	520	43.7	1110	11.3	288	8.25, 7.50	12.5	318	473	6610	105	3000	720	6005	105	2725	720
11R24.5	H	79250	24	65	20.5	520	43.7	1111	11.4	289	8.25, 7.50	12.5	318	473	7160	120	3250	830	6610	120	3000	830

Spécifications pour bandes de roulement: XDA-HT™ High Torque

Dimension	Gamme de charge	Numéro de catalogue	Profondeur de bande de roulement (32e)	Vitesse maximale (mi/h)	Rayon sous charge		Diamètre hors tout		Largeur hors tout		Jantes approuvées	Entraxe min. entre jumelés		Tours/mille	Charge maximale (pneus simples)				Charge maximale (pneus jumelés)			
					po	mm	po	mm	po	mm		po	mm		lb	psi	kg	kPa	lb	psi	kg	kPa
11R22.5	G	93430	30	75	19.6	497	41.9	1065	11.2	284	8.25, 7.50	12.5	318	494	6175	105	2800	720	5840	105	2650	720
275/80R22.5	G	50575	30	75	19.1	484	40.8	1035	11.0	278	8.25, 7.50	12.2	311	508	6175	110	2800	760	5675	110	2575	760
11R24.5	H	59777	30	75	20.6	523	43.8	1112	11.2	285	8.25, 7.50	12.5	318	471	7160	120	3250	830	6610	120	3000	830
11R24.5	G	81937	30	75	20.6	523	43.8	1112	11.2	285	8.25, 7.50	12.5	318	471	6610	105	3000	720	6005	105	2725	720
275/80R24.5	G	55519	30	75	19.7	501	42.0	1066	10.7	272	8.25, 7.50	12.2	311	492	6175	110	2800	760	5675	110	2575	760

Tire and pressure characteristics

		Tire Position	Tire Size	Tire Maker	Tire Model	Pressure normal/reduced (psi)
Steer	1	L Steer	11R24.5	Michelin	XZE LRH	100/100
	2	R Steer	11R24.5	Michelin	XZE LRH	100/100
Drives	3	Drive 1 L-O	11R24.5	Michelin	XDHT LRG	100/60
	4	Drive 1 L-I	11R24.5	Michelin	XDHT LRG	100/60
	5	Drive 1 R-I	11R24.5	Michelin	XZE LRG	100/60
	6	Drive 1 R-O	11R24.5	Michelin	XZY-2 LRG	100/60
	7	Drive 2 L-O	11R24.5	Michelin	XDHT LRG	100/60
	8	Drive 2 L-I	11R24.5	Michelin	XDY-2 LRG	100/60
	9	Drive 2 R-I	11R24.5	Michelin	XDN2 LRG	100/60
	10	Drive 2 R-O	11R24.5	Michelin	XZA-1 LRG	100/60
Trailer	19	Tridem 2 L-O	11R24.5	Michelin	XDA-HT LRG	100/55
	20	Tridem 2 L-I	11R24.5	Michelin	XDA-HT LRG	100/55
	21	Tridem 2 R-I	11R24.5	Michelin	XZY3 LRH	100/55
	22	Tridem 2 R-O	11R24.5	Michelin	XZY3 LRH	100/55
	23	Tridem 3 L-O	11R24.5	Michelin	XZE LRG	100/55
	24	Tridem 3 L-I	11R24.5	Michelin	XDA-HT LRH	100/55
	25	Tridem 3 R-I	11R24.5	Michelin	XDA-HT LRH	100/55
	26	Tridem 3 R-O	11R24.5	Michelin	XDA-HT LRG	100/55
	27	Tridem 4 L-O	11R24.5	Michelin	XDS LRH	100/55
	28	Tridem 4 L-I	11R24.5	Firestone	FD663	100/55
	29	Tridem 4 R-I	11R24.5	Yokohama	RY637 LRG	100/55
	30	Tridem 4 R-O	11R24.5	Sumitomo	ST928 LRH	100/55

Wide tire	455/55R22.5 LRL	Michelin	X one	80/100/120 psi
------------------	------------------------	-----------------	--------------	-----------------------

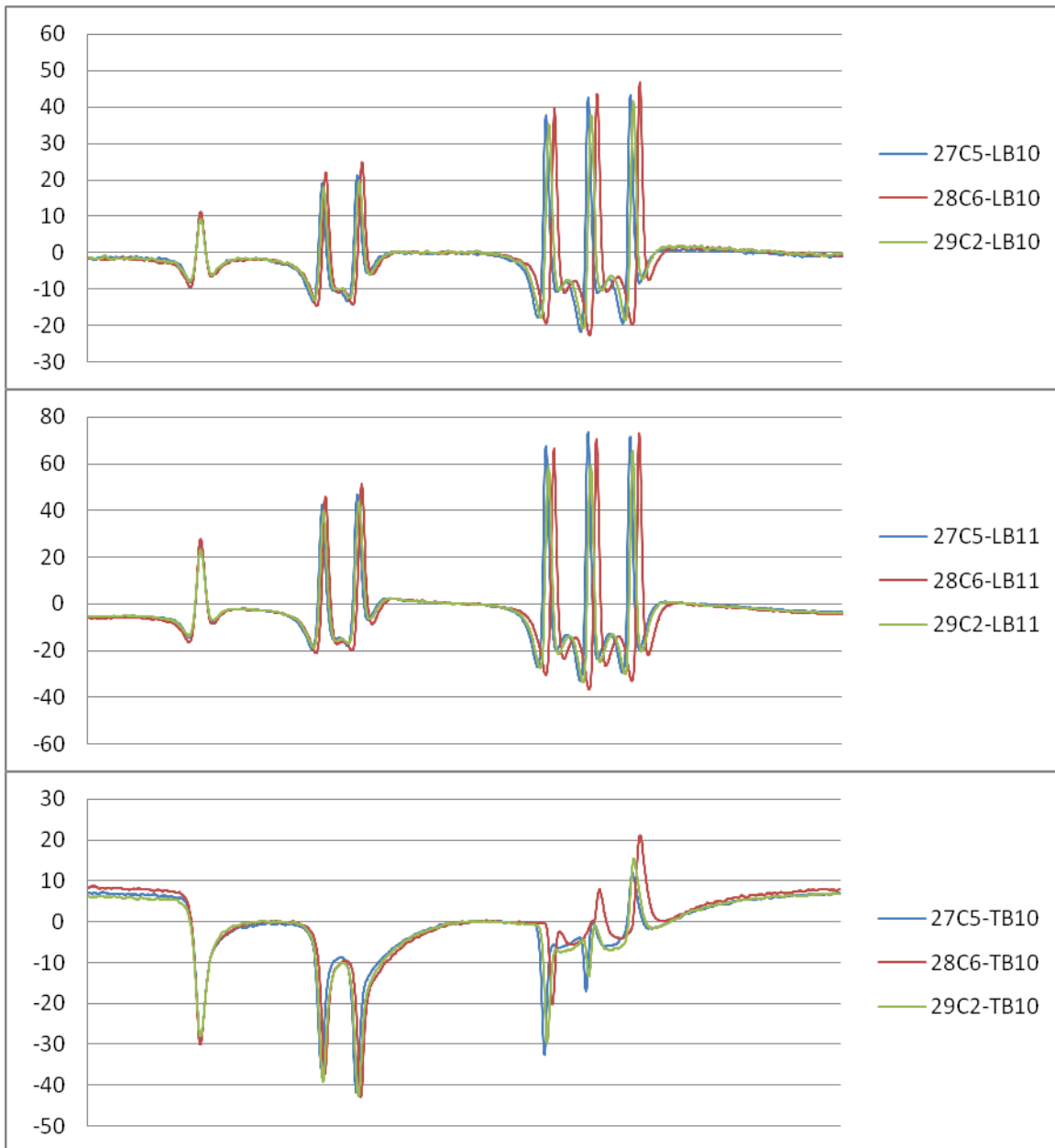
ANNEX 2. *Trials matrix*

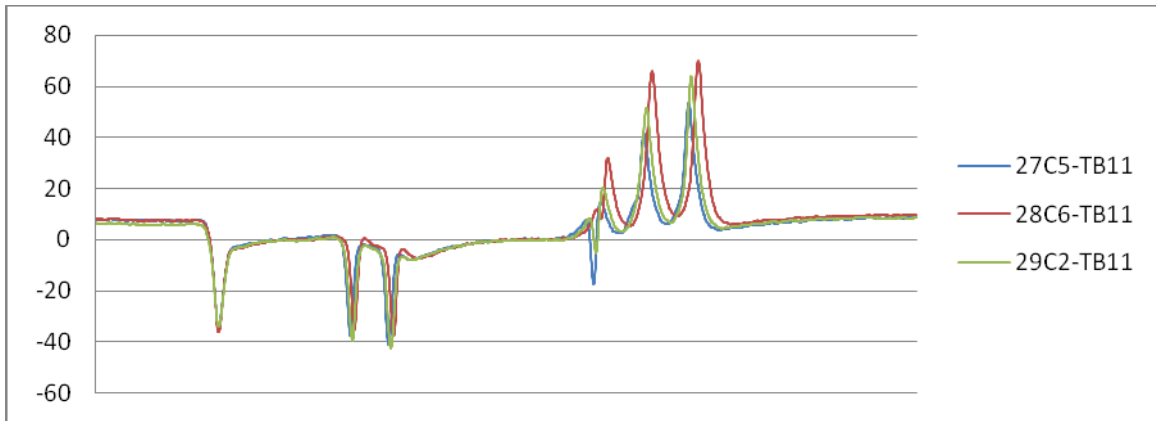
Trial number	Asphalt thickness	Pressure in steer tires	Pressure in drives tires	Pressure in trailer tires	Type of tire	Name
15	100	100	60	55	Double	15C
16	Enduit	100	60	55	Double	16C
17	Enduit	100	100	100	Double	17C
18	50	100	100	100	Double	18C
19	50	100	60	55	Double	19C
20	50	100	100	120	Large	20C
21	50	100	100	100	Large	21C
22	50	100	75	80	Large	22C
23	Enduit	100	120	100	Large	23C
24	Enduit	100	100	100	Large	24C
25	Enduit	100	100	80	Large	25C
26	Enduit	100	100	120	Large	26C
27	100	100	100	120	Large	27C
28	100	100	100	100	Large	28C
29	100	100	100	80	Large	29C

ANNEX 3. *Test results*

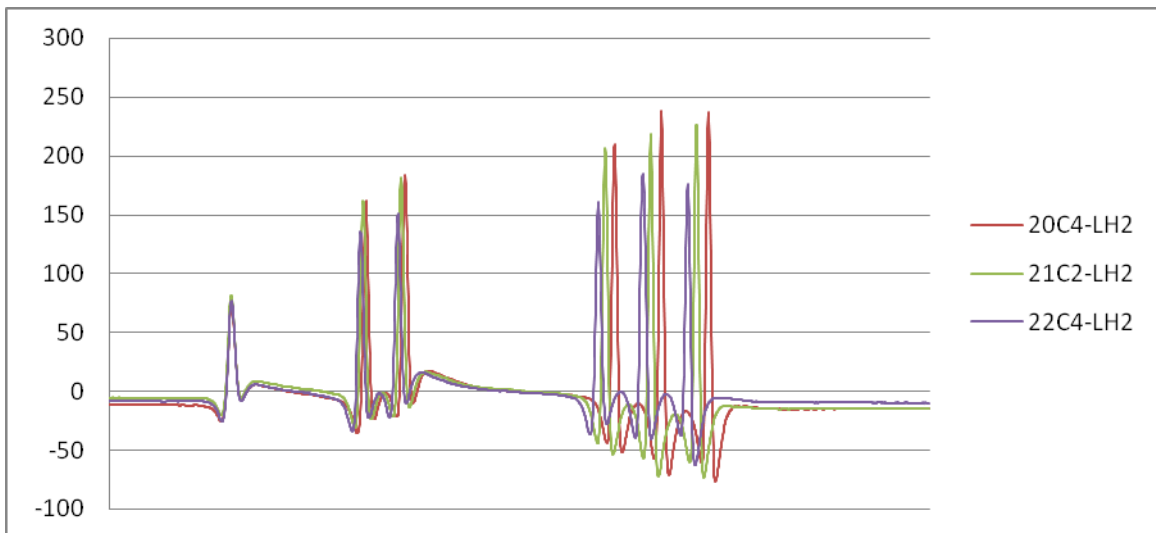
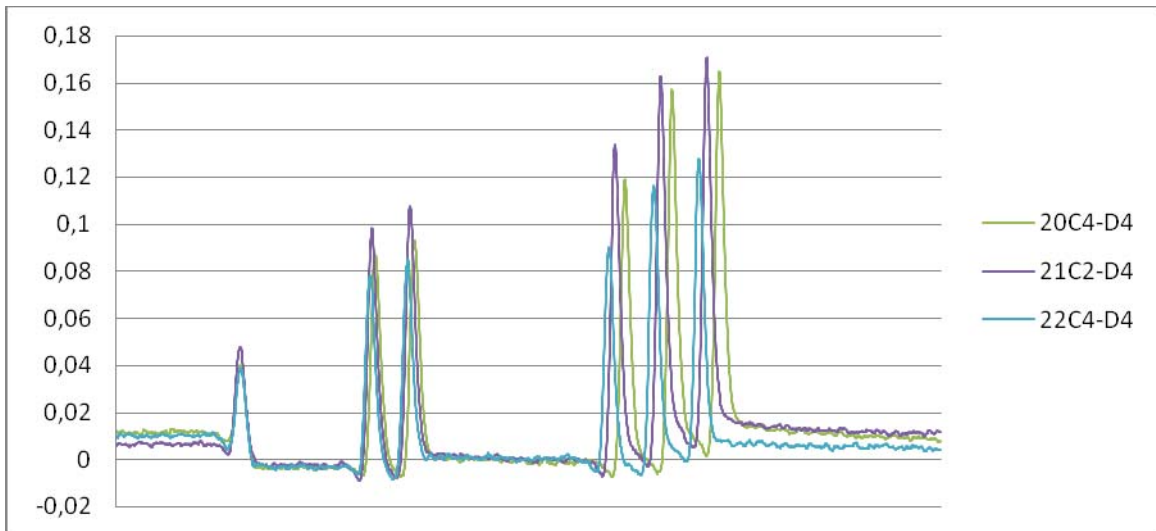
The following figures show the results of all selected test pass. On the 100 mm section (27C, 28C, 29C) and the 50 mm section (20C, 21C, 22C), results for each pressure layout are presented in a same graph. Only deflection is given for the surface treated section.

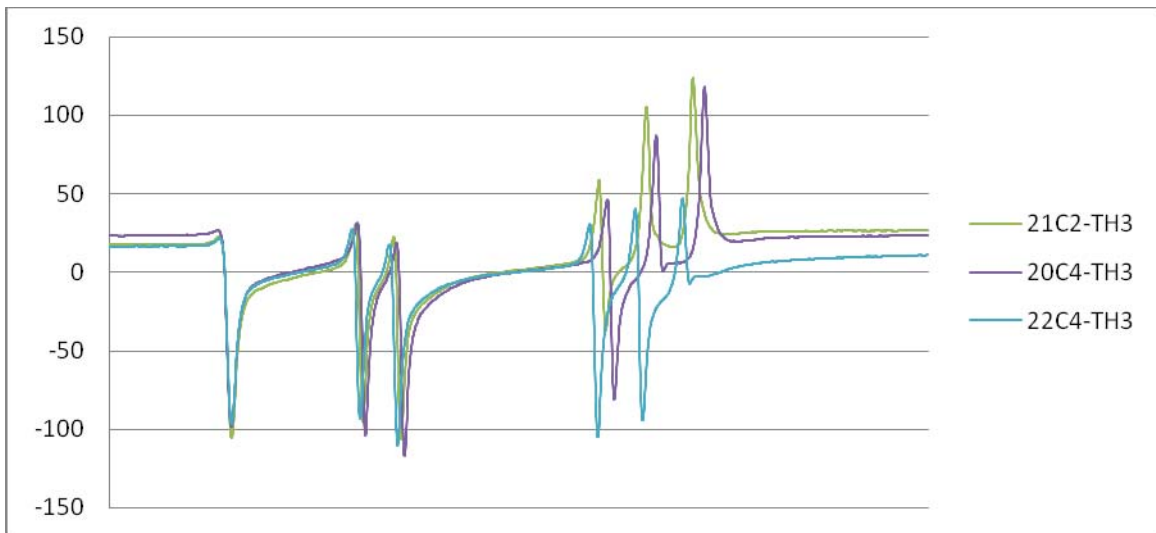
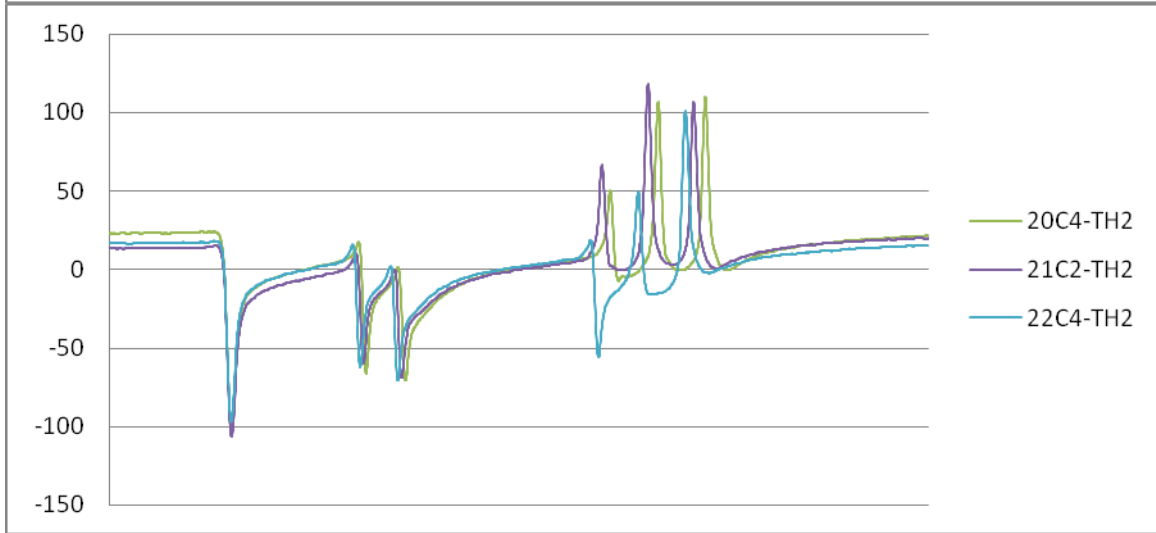
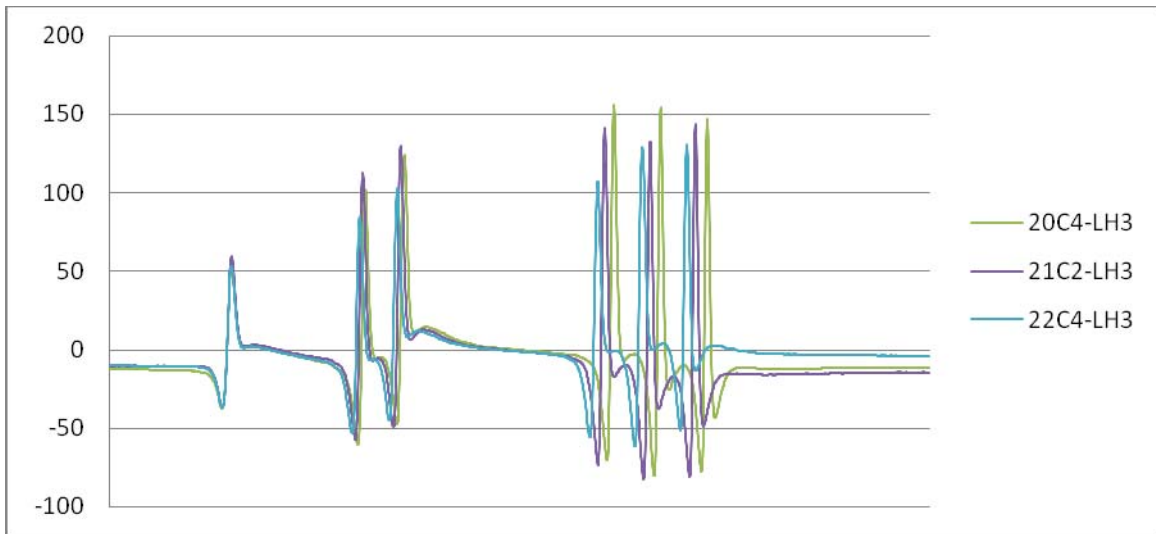
Thickness of 100 mm





Thickness of 50 mm





Surface treatment

